PH4201: Adv. Optics Lab Report

Observation of Pancharatnam-Berry Phase in Polarized Light

Debayan Sarkar	Sabarno Saha	Diptanuj Sarkar
Roll No: 22MS002	Roll No: 22MS037	Roll No: 22MS038

Date: 26 February 2026

1. Aim

In this experiment, we will use the Michelson Interferometer to demonstrate the Pancharatnam-Berry phase in polarized light.

2. Materials required

1. Collimated Laser Source(wavelength: 650 nm)
2. Two Quarter-Wave Plates and one linear polariser
3. Two mirrors
4. Beam Splitter
5. Biconvex Lenses

3. Theory

The experimental setup to observe the Pancharatnam-Berry phase in polarized light is based on a Michelson interferometer. The interferometer consists of a beam splitter that divides the incoming light into two paths. The uniformly polarized light from the laser source is first passed through a linear polarizer. In one of the arms of the interferometer, there are two quarter waveplates. The first quarter waveplate is fixed at an angle of 45^o with respect to the polarization direction of the incoming light, while the second quarter waveplate can be rotated by an angle of β with respect to the first one.

The linear polarizer is rotated to maximise the internsity of light entering the beam splitter. The QP1 is aligned with $\frac{\pi}{4}$ with respect to the polarization direction of the incoming light, which is ensured by rotating until the fringes disappear. The second QWP is rotated by an angle of β and the fringe shifts are counted.

At the end of the interferometer, the light is passed through a biconvex lens to focus the light onto a screen where the interference pattern can be observed. The interference pattern will shift as the angle β of the second quarter waveplate is varied, allowing us to observe the effect of the Pancharatnam-Berry phase on the interference pattern.

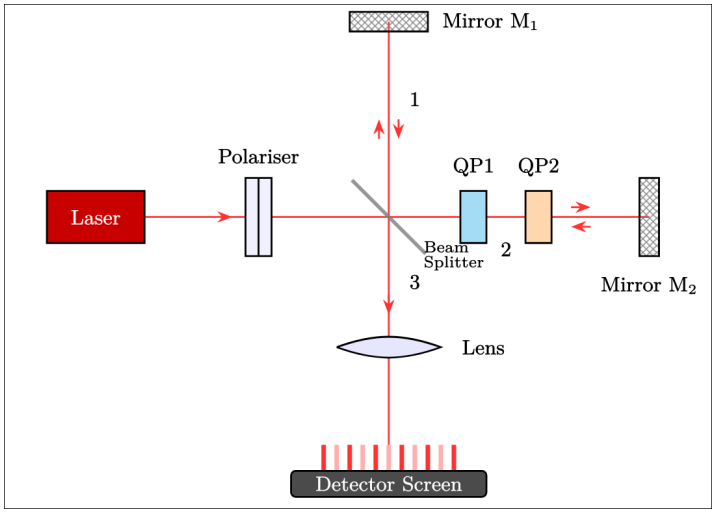

Figure 1: Experiment Setup for a Michelson Interferometer, to observe the Pancharatnam-Berry phase in polarized light.

3.1. Poincare Sphere Representation

The Poincaré sphere is a powerful tool for visualizing the polarization states of light. Each point on the surface of the sphere represents a unique polarization state. The equator of the sphere corresponds to linear polarization states, while the poles correspond to circular polarization states. The points in between represent elliptical polarization states. The Poincaré sphere allows us to understand how the polarization state of light changes as it passes through different optical elements, such as waveplates and polarizers. The Pancharatnam-Berry phase can be visualized on the Poincaré sphere as a geometric phase acquired by the polarization state of light as it undergoes a cyclic evolution on the sphere.

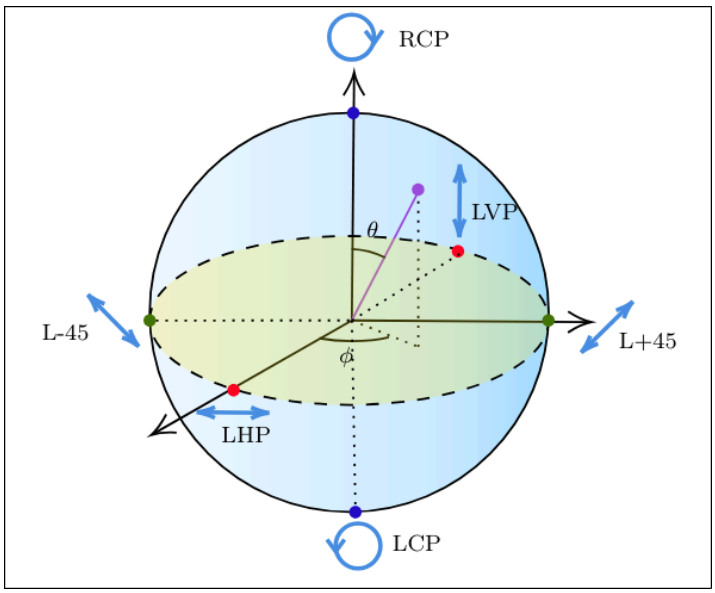

Figure 2: Poincaré sphere representation of the polarization states of light.

3.2. Jones Matrix Formalism

The Jones matrix formalism helps us understand the effect of the optical elements on the polarization state of light. The Jones vector for a linearly polarized light can be represented as:

$$\boldsymbol{E} = \begin{pmatrix} 1 \\ 0 \end{pmatrix} \tag{3.1}$$

Here we consider the x-axis to be the direction of polarization. The effect of a quarter waveplate with an angle of θ can be represented by the following Jones matrix:

$$J_{\mathrm{QWP}}(\theta) = \begin{pmatrix} \cos^2(\theta) + i\sin^2(\theta) & (1-i)\cos(\theta)\sin(\theta) \\ (1-i)\cos(\theta)\sin(\theta) & \sin^2(\theta) + i\cos^2(\theta) \end{pmatrix} \tag{3.2}$$

For a quarter waveplate with its fast axis at 45^o, the Jones matrix simplifies to:

$$J_{\mathrm{QWP}}(45^o) = \frac{1}{\sqrt{2}} \begin{pmatrix} 1+i & 1-i \\ 1-i & 1+i \end{pmatrix} \tag{3.3}$$

Thus after passing through the first quarter waveplate, the Jones vector for the linearly polarized light,upto a dynamical phase becomes:

$$\boldsymbol{E}_1 = J_{\mathrm{QWP}}(45^o)\boldsymbol{E} = \frac{1}{\sqrt{2}} \begin{pmatrix} 1+i & 1-i \\ 1-i & 1+i \end{pmatrix} \begin{pmatrix} 1 \\ 0 \end{pmatrix} = \frac{1}{2} \begin{pmatrix} 1+i \\ 1-i \end{pmatrix} = \frac{1+i}{2} \begin{pmatrix} 1 \\ -i \end{pmatrix} \tag{3.4}$$

Then it passes through the second quarter waveplate, which is rotated by an angle of β with respect to the first one. The Jones vector after passing through the second quarter waveplate is given by:

$$\begin{aligned} \boldsymbol{E}_2 &= J_{\mathrm{QWP}}(\beta)\boldsymbol{E}_1 = J_{\mathrm{QWP}}(\beta)J_{\mathrm{QWP}}(45^o)\boldsymbol{E} \\ &= \begin{pmatrix} \cos^2(\beta) + i\sin^2(\beta) & (1-i)\cos(\beta)\sin(\beta) \\ (1-i)\cos(\beta)\sin(\beta) & \sin^2(\beta) + i\cos^2(\beta) \end{pmatrix} \frac{1+i}{2} \begin{pmatrix} 1 \\ -i \end{pmatrix} \end{aligned} \tag{3.5}$$

Then it reflects off the mirror which induces a phase shift of π on the electric field. Thus the Jones vector after reflection is given by:

$$\boldsymbol{E}_3 = \begin{pmatrix} 1 & 0 \\ 0 & -1 \end{pmatrix} \boldsymbol{E}_2 \tag{3.6}$$

After passing through the second quarter waveplate again, the Jones vector becomes:

$$\boldsymbol{E}_4 = J_{\mathrm{QWP}}(\beta)\boldsymbol{E}_3 \tag{3.7}$$

Finally, after passing through the first quarter waveplate again, the Jones vector becomes:

$$\boldsymbol{E}_5 = J_{\mathrm{QWP}}(45^o)\boldsymbol{E}_4 \tag{3.8}$$

At the end of the interferometer, the light is projected onto the original polarization state using a polarizer. The Jones vector after projection is given by:

$$\boldsymbol{E}_f = e^{-i\varphi}e^{-2i\beta} \begin{pmatrix} 1 \\ 0 \end{pmatrix} \tag{3.9}$$

where φ is the dynamical phase acquired during the propagation of light through the interferometer, which does not change unless the elements of the interferometer are changed. The Pancharatnam-Berry phase is given by the geometric phase $e^{-2i\beta}$. For interference to occur, the final state must be the same as the initial state, which means that the total phase difference between the two paths must be an integer multiple of 2π. Thus, the condition for constructive interference is given by:

$$\varphi + 2\beta = 2n\pi, n \in Z \tag{3.10}$$

Since the mirrors, beam spitters and waveplates are all static, the dynamical phase φ remains constant. Therefore, by varying the angle β of the second quarter waveplate, we can observe the interference pattern and see the effect of the Pancharatnam-Berry phase on the interference.

4. Results and Analysis

We used three different data sets to analyze the relationship between the fringe shift and the angle β of the second quarter waveplate. The last data set was taken by switching the positions of the two quarter waveplates, which should not affect the results as the Pancharatnam-Berry phase is a geometric phase and does not depend on the specific path taken by the light. It should also not change the dynamical phase, since the optical elements are the same, just in a different order. The reason for this is because the second QWP is more tilted with respect to the vertical axis. It also had a higher reflection coefficient, which causes more wavefronts to interfere with each other. And moving the second QWP to the first position causes the wavefronts to shift anomalously and the fringe shift is more erroneous.

One can also see this from the plot, where the slope fit error is lower for the last data set compared to the first two data sets. The results from all three data sets are in good agreement with the theoretical prediction of a slope of 2 for the fringe shift vs β plot, confirming the presence of the Pancharatnam-Berry phase in our experimental setup.

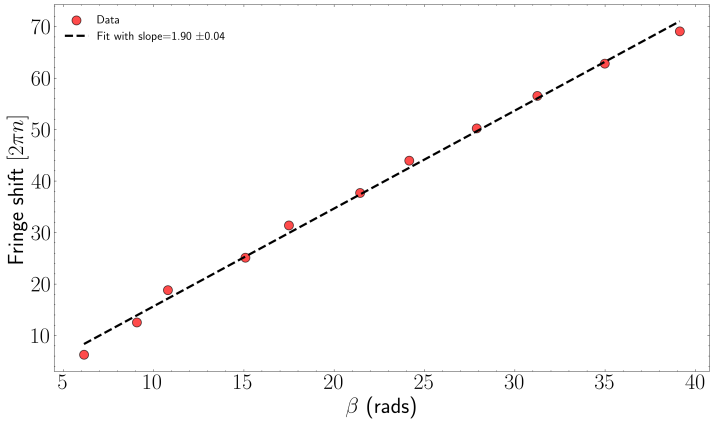

Figure 3: Fringe shift vs β for Data Set 1. The slope of the fit is 1.90 ± 0.04, which is in good agreement with the theoretical prediction of 2.

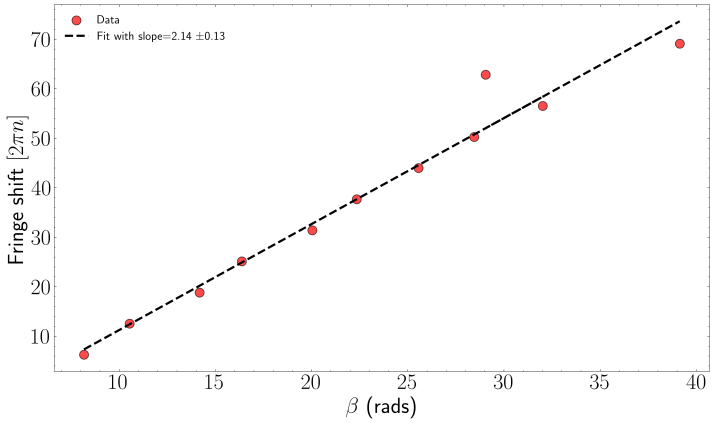

Figure 4: Fringe shift vs β for Data Set 2. The slope of the fit is 2.14 ± 0.13, which is in good agreement with the theoretical prediction of 2.

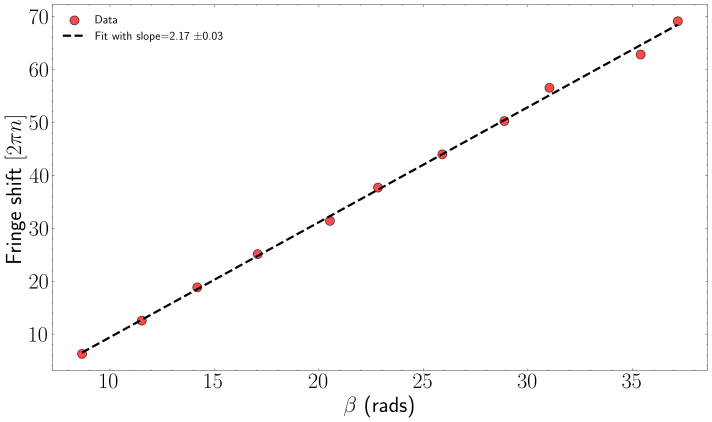

Figure 5: Fringe shift vs β for Data Set 3. The slope of the fit is 2.17 ± 0.03, which is in good agreement with the theoretical prediction of 2.

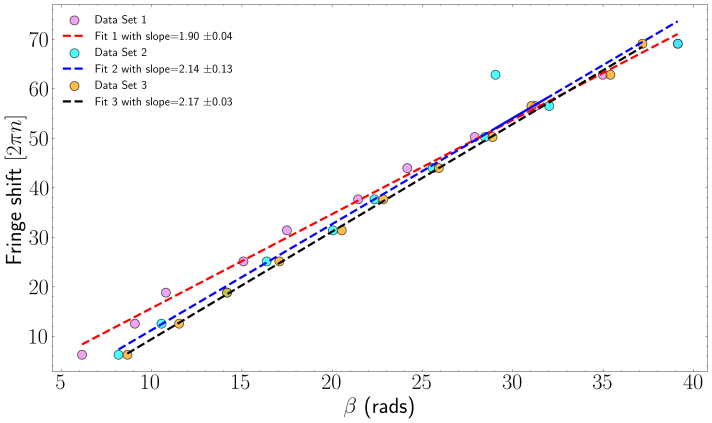

Figure 6: Fringe shift vs β for all three data sets. The slopes of the fits are 1.90 ± 0.04, 2.14 ± 0.13, and 2.17 ± 0.03 for Data Sets 1, 2, and 3 respectively, all of which are in good agreement with the theoretical prediction of 2.

5. Error Analysis

Since the theoretical prediction is a slope of 2 for the fringe shift vs β plot, we can calculate the percentage error for each data set using the formula:

$$\begin{aligned} \delta_1 &= \left|\frac{1.90-2}{2}\right| 100 = 5\% \\ \delta_2 &= \left|\frac{2.14-2}{2}\right| 100 = 7\% \\ \delta_3 &= \left|\frac{2.17-2}{2}\right| 100 = 8.5\% \end{aligned} \tag{5.1}$$

5.1. Maximum possible error

The maximum possible error in the slope can be calculated using the least count. The least count of the angle β is 2°, which is approximately 0.035 radians. Since the least count of the fringe shift is 1. The error calculation,

$$\delta_{\max} = \sqrt{\left(\frac{\delta n}{n}\right)^2 + \left(\frac{\delta \beta}{\beta}\right)^2} \approx 1.003 \tag{5.2}$$

The minimum n is 1 and the minimum β is 5.4 radians. Thus the maximum possible error in the slope is approximately 1.003.

5.2. Sources of error

1. The Michelson Interferometer is very sensitive to vibrations and air currents, which can cause the interference pattern to shift and make it difficult to obtain clear fringes. This can lead to errors in counting the fringe shifts.
2. The beam splitter causes inadvertent reflections, which can interfere with the main beams and cause additional fringes that can be mistaken for the main interference pattern. This can again lead to errors in counting the fringe shifts.
3. The quarter waveplates may not be perfectly aligned, which can affect the polarization state of the light and lead to errors in the observed fringe shifts. This can be mitigated by carefully aligning the quarter waveplates and ensuring that they are at the correct angles.
4. One of the quarter waveplates is more tilted with respect to the vertical axis, which causes more wavefronts to interfere with each other and can lead to anomalous fringe shifts. This can be mititgated by fixing the quarter waveplate and not rotating it, and instead rotating the other quarter waveplate to vary the angle β.
5. Impurities and scratches on the beam splitter distort fringe visibility and can lead to errors in counting the fringe shifts. This can be mitigated by using a clean and high-quality beam splitter.

6. Conclusion

The Pancharatnam-Berry phase is a geometric phase that arises in polarized light when it undergoes a cyclic evolution in the polarization state. In this experiment, we used a Michelson Interferometer to demonstrate the presence of the Pancharatnam-Berry phase in polarized light. We observed that the fringe shift in the interference pattern is proportional to the angle β of the second quarter waveplate. The proportionality constant was found to be $1.90 \pm 0.04, 2.14 \pm 0.13$ and 2.17 ± 0.03 for the three data sets, which is in good agreement with the theoretical prediction of 2.

7. Discussion

One way to improve the experiment would be to use a more stable setup that is less sensitive to vibrations and air currents. This could involve using a Mach Zender Interferometer instead of a Michelson Interferometer, as the Mach Zender Interferometer is less sensitive to vibrations and air currents. Additionally, using a more stable platform for the interferometer and isolating it from external vibrations could also help improve the results. However, this would cause an issue, we would require two more quarter waveplates. Two pairs of quarter waveplates have to be in sync with each other, since the light has to virtually retrace its path after hitting the mirror in the Mach Zender Interferometer, which can be difficult to achieve in practice. The Michelson Interferometer, on the other hand, only requires one pair of quarter waveplates, where the light already retraces its path after hitting the mirror, which makes it easier to set up and align. Thus, while using a Mach Zender Interferometer could potentially improve the stability of the experiment, it would also introduce additional complexities in terms of alignment and synchronization of the quarter waveplates.

One could also use better quarter waveplates, ones with lower reflecton coefficients and better quality, to reduce the anomalous fringe shifts caused by the tilted quarter waveplate.

One anomaly that we observed was that the fringe shifts were not completely linear with respect to the angle β of the second quarter waveplate. Periodically, the fringes would move in the opposite direction slightly before continuing to shift in the expected direction. However, these slight variations

are not resolvable in the plot since these happen periodically and are smoothened out. We still do not know why this happens, but it could be due to the fact that the second quarter waveplate is more tilted with respect to the vertical axis.

8. Supplementary Data

Set 1 Data

β(in deg.)	β(in rad)	fringe shift
184	3.211405824	0
352	6.143558967	1
520	9.07571211	2
618	10.78613478	3
864	15.07964474	4
1002	17.4881991	5
1228	21.43264321	6
1384	24.15535685	7
1598	27.89036145	8
1790	31.24139361	9
2004	34.97639821	10
2242	39.13028183	11
2410	42.06243497	12
2640	46.07669225	13
2780	48.52015321	14
3022	52.74385	15

Set 2 Data

β (in deg.)	β (in rad.)	fringe shift
314	5.480333851	0
468	8.168140899	1
604	10.54178868	2
812	14.17207353	3
938	16.37118838	4
1148	20.03637981	5
1280	22.34021443	6
1464	25.55162025	7
1630	28.44886681	8
1834	32.00933848	9
1664	29.04227875	10
2242	39.13028183	11
2412	42.09734156	12
2628	45.86725274	13
2744	47.89183467	14

2906	50.71926806	15

Set 3 Data

β (in deg.)	β (in rad.)	fringe shift
296	5.166174586	0
496	8.65683309	1
660	11.51917306	2
812	14.17207353	3
978	17.06932008	4
1176	20.525072	5
1308	22.82890662	6
1484	25.9006861	7
1654	28.86774583	8
1778	31.0319541	9
2028	35.39527723	10
2130	37.17551307	11
2248	39.23500158	12
2418	42.20206131	13
2564	44.75024202	14
2698	47.08898322	15